9. Mottram CJ, Jakobi JM, Semmler JG, Enoka RM. Motor-unit activity differs with load type during a fatiguing contraction. *J Neurophysiol*. 2005;93:1381-1392.

SUPPORTING INFORMATION

Additional supporting information may be found online in the Supporting Information section at the end of this article.

How to cite this article: Posa A, Niśkiewicz I, Raescu V, Emmer A, Surov A, Kornhuber M. Spontaneous continuous motor unit single discharges. *Muscle Nerve*. 2020;61:383–400. https://doi.org/10.1002/mus.26789

Examination of the human motor endplate after brachial plexus injury with two-photon microscopy

Justin P. Chan BA[1] | James Clune MD[2] | Sameer B. Shah PhD[3,4] | Samuel R. Ward PhD[3,4] | Jeffery D. Kocsis PhD[5] | Tahseen Mozaffar MD[6] | Oswald Steward PhD[7] | Ranjan Gupta MD[1]

[1]Department of Orthopaedic Surgery, University of California, Irvine, Irvine, California

[2]Section of Plastic and Reconstructive Surgery, Yale University School of Medicine, New Haven, Connecticut

[3]Department of Orthopaedic Surgery, University of California, San Diego, La Jolla, California

[4]Department of Bioengineering, University of California, San Diego, La Jolla, California

[5]Department of Neurology, Yale University School of Medicine, New Haven, Connecticut

[6]Department of Neurology, University of California, Irvine, Irvine, California

[7]Reeve-Irvine Research Center, University of California, Irvine, Irvine, California

Correspondence
Ranjan Gupta, Department of Orthopaedic Surgery, 2226 Gillespie Neuroscience Research Facility, University of California, Irvine, 837 Health Science Road, Irvine, CA 92697.
Email: ranjang@uci.edu

Abstract

Introduction: After traumatic nerve injury, neuromuscular junction remodeling plays a key role in determining functional outcomes. Immunohistochemical analyses of denervated muscle biopsies may provide valuable prognostic data regarding clinical outcomes to supplement electrodiagnostic studies.

Methods: We performed biopsies on nonfunctioning deltoid muscles in two patients after gunshot wounds and visualized the neuromuscular junctions using two-photon microscopy with immunohistochemistry.

Results: Although the nerves in both patients showed evidence of acute Wallerian degeneration, some of the motor endplates were intact but exhibited significantly decreased surface area and volume. Both patients exhibited substantial recovery of motor function over several weeks postinjury.

Discussion: Two-photon microscopic assessment of neuromuscular junction integrity and motor endplate morphometry in muscle biopsies provided evidence of partial sparing of muscle innervation. This finding supported the clinical judgment that eventual recovery would occur. With further study, this technique may help to guide operative decisionmaking after traumatic nerve injuries.

KEYWORDS

brachial plexus injury, gunshot wound, motor endplate, neuromuscular junction, traumatic nerve injury

1 | INTRODUCTION

After brachial plexus injuries (BPIs), some patients have spontaneous recovery, whereas others require surgical intervention to improve their functional outcome.[1,2] Formulating diagnostic criteria to identify patients who may benefit from surgery is a high priority. Magnetic resonance imaging and ultrasound are both useful for identifying damaged nerves preoperatively, but they cannot predict regeneration potential,[3-5] which depends on the viability of the motor endplate (MEP) within targeted muscle fibers.[6]

Abbreviations: BPI, brachial plexus injury; H&E, hematoxylin and eosin; MEP, motor endplate; MRC, Medical Research Council; NF, neurofilament; NMJ, neuromuscular junction.

Without definitive diagnosis of nerve transection and with an inability to track viability of the neuromuscular junction (NMJ), many surgeons delay surgery to assess spontaneous recovery and avoid unnecessary or potentially detrimental procedures.[7] As human nerves grow at a rate of ~1 mm/day, it often requires months before clinical signs of regeneration are apparent.[8] However, late surgical intervention risks irreversible degradation of the target end-organ, thus missing the critical window during which functional recovery is achievable.[9,10]

To develop tools for predicting spontaneous neuromuscular recovery, there is a crucial need for a deeper understanding of the fate of human MEPs after denervation. Animal models predict that partial preservation of the NMJ may be a useful prognostic indicator for eventual nerve regeneration. Such information could be especially valuable if comprised of quantitative morphometric measures of NMJ remodeling. Given the lack of human data in this area, we describe an approach to visualize NMJs in muscle biopsies.

2 | METHODS

2.1 | Case reports

Two young, healthy males, ages 26 and 23 years, sustained similar gunshot wounds to the right upper extremity within minutes of each other during a mass casualty incident. Both patients had BPIs, including complete motor and sensory loss in the right axillary nerve distribution without transection injury, and required standard-of-care surgery to address their bony injuries where the deltoid muscle was readily accessible. After receiving institutional review board approval and obtaining informed consent, the right deltoid muscle was biopsied in these patients at 3 weeks and 5 months, respectively, allowing comparison with a control deltoid biopsy from another subject undergoing upper extremity surgery unrelated to a nerve injury.

2.2 | Muscle processing and analysis

Muscle samples were fixed in 4% paraformaldehyde, separated into longitudinal whole mounts,[11] and immunostained with antibodies to NMJ components as follows: 1) α-bungarotoxin (Alexa Fluor 594 conjugate; 1/1000; ThermoFisher Scientific) to label nicotinic acetylcholine receptors; 2) synaptophysin to label presynaptic vesicles (mouse anti-human synaptophysin; 1/250; Dako); and 3) neurofilament (NF) to label axons (mouse anti-human NF; 1/300; Covance). Secondary antibodies were conjugated to donkey anti-mouse Alexa Fluor 488 (1/300; ThermoFisher Scientific). Two-photon images were acquired with a 3i system (Intelligent Imaging Innovations) with an 810-nm laser and Zeiss 20x/0.8 water immersion objective. Three-dimensional reconstructions were created (Volocity, Perkin Elmer). MEP surface area/volume were quantified using ImageJ (National Institutes of Health) with the 3D Object Counter plug-in using the optical fractionator method.

TABLE 1A Patient 1: Sensory nerve conduction data

Nerve	Recording site	Peak latency (ms)	Amplitude (μV)	Velocity (m/s)	Normal values
Right median					Peak latency 3.5 ms, amplitude 20 μV
Wrist	Digit II	No response	No response	No response	
Right ulnar					Peak latency 3.1 ms, amplitude 17 μV
Wrist	Digit V	No response	No response	No response	
Right radial					Peak latency 2.9 ms, amplitude 15 μV
Forearm	Wrist	No response	No response	No response	

TABLE 1B Patient 1: Motor nerve conduction data

Nerve	Muscle	Latency (ms)	Amplitude (mV)	Velocity (m/s)	Normal values
Right median					Distal latency 4.4 ms, amplitude 4.0 mV, velocity 50 m/s
Wrist	APB	No response	No response	No response	
Right ulnar					Distal latency 3.3 ms, amplitude 6.0 mV, velocity 50 m/s
Wrist	ADM	3.44	1.3		
Below elbow	ADM	7.71	1.3	56	
Above elbow	ADM	8.91	1.3	75	
Right radial					Amplitude 2.0 mV, velocity 50 m/s
Forearm	EIP	9.38	0.2		
Elbow	EIP	10.36	0.2	76	
Arm	EIP	12.71	0.2	47	

Abbreviations: ADM, abductor digiti minimi; APB, abductor pollicis brevis; EIP, extensor indicis proprius.

TABLE 1C Patient 1: Electromyography data

	Spontaneous		Volitional MUAPs		
Muscle	Fibs/PSW	Fasciculations	Duration	Amplitude	Recruitment
Right abductor digit minimi	1^+	None	Normal	Normal	Moderately decreased
Right extensor digitorum communis	3^+	None	Normal	Normal	Markedly decreased
Right triceps brachii	1^+	None	Normal	Normal	Moderately decreased
Right deltoid	None	None	Normal	Normal	Mildly decreased
Right biceps brachii	None	None	Normal	Normal	Mildly decreased
Right abductor pollicis brevis	None	None	No motor units	No motor units	

Abbreviations: ADM, abductor digiti minimi; APB, abductor pollicis brevis; EIP, extensor indicis proprius; Fibs/PSW, fibrillation potentials/positive sharp waves; MUAP, motor unit action potential.

TABLE 2A Patient 2: Sensory nerve conduction data

Nerve	Recording site	Peak latency (ms)	Amplitude (μV)	Velocity (m/s)	Normal values
Right median					Peak latency 3.5 ms, amplitude 20 μV
Wrist	Digit II	3.13	52.2	71	
Right ulnar					Peak latency 3.1 ms, amplitude 17 μV
Wrist	Digit V	2.97	31.3	49	
Right radial					Peak latency 2.9 ms, amplitude 15 μV
Forearm	Wrist	2.03	6.5	69	
Left radial					Peak latency 2.9 ms, amplitude 15 μV
Forearm	Wrist	2.14	22.5	62	

TABLE 2B Patient 2: Motor nerve conduction data

Nerve	Muscle	Latency (ms)	Amplitude (mV)	Velocity (m/s)	Normal values
Right median					Distal latency 4.4 ms, amplitude 4.0 mV, velocity 50 m/s
Wrist	APB	3.54	10.0		
Elbow	APB	7.60	9.7	54	
Right ulnar					Distal latency 3.3 ms, amplitude 6.0 mV, velocity 50 m/s
Wrist	ADM	2.40	13.0		
Below elbow	ADM	6.35	12.6	58	
Above elbow	ADM	8.39	11.9	54	
Right radial					Amplitude 2.0 mV, velocity 50 m/s
Forearm	EIP	No response	No response	No response	

Abbreviations: ADM, abductor digiti minimi; APB, abductor pollicis brevis; EIP, extensor indicis proprius; Fibs/PSW, fibrillation potentials/positive sharp waves; MUAP, motor unit action potential.

Hematoxylin-and-eosin (H&E) staining was used to visualize muscle fiber architecture in transverse cryosections of fresh frozen muscle.

3 | RESULTS

Electrodiagnostic studies were performed on patients 1 and 2 at 4 weeks after injury, demonstrating indicating deficits in the distribution of the right median, ulnar, radial, and axillary nerves in patient 1 (Tables 1A-C), and in the right axillary and radial nerve distributions in patient 2 (Table 2A-C).

On H&E staining (Figure 1), patient 1 demonstrated highly variable muscle fiber diameters with diffuse, dense cellular infiltrate throughout the specimen, consistent with early myofiber regeneration. In contrast, patient 2 demonstrated uniform fiber diameters, indicating normal muscle morphology. Neither specimen exhibited changes typical of late-stage muscle injury (adipocyte infiltration or collagen deposition).

The deltoid biopsy from patient 1 (3 weeks postinjury) showed extensive neurofilament debris scattered throughout the field compared with the control specimen, indicating active Wallerian degeneration (Figure 1E). The biopsy from patient 2 (5 months

TABLE 2C Patient 2: Electromyography data

	Spontaneous		Volitional MUAPs		
Muscle	**Fibs/PSW**	**Fasciculations**	**Duration**	**Amplitude**	**Recruitment**
Right triceps brachii	2^+	None	Normal	Normal	Moderately decreased
Right brachioradialis	None	None	Rare motor units		Markedly decreased
Right extensor indicis proprius	3^+	None	No motor units	No motor units	
Right deltoid	2^+	None	Normal	Normal	Reduced
Right biceps brachii	None	None	Normal	Normal	Normal
Right first dorsal interosseous	None	None	Normal	Normal	Normal

Abbreviations: Fibs/PSW, fibrillation potentials/ positive sharp waves; MUAP, motor unit action potential.

postinjury) also showed neuronal debris, consistent with late Wallerian degeneration. In both patients, the synaptophysin signal was in contact with some, but not all, MEPs (white arrowheads in Figure 1E-F). MEPs of both patients were grossly intact but showed marked condensation with loss of infoldings compared with controls, an 86% reduction of surface area (Figure 2), and decreases in endplate volume of 53% and 49% for patients 1 and 2, respectively.

Patient 1 started to regain both motor and sensory functions in the distribution of the axillary nerve at 6 months postinjury, and eventually regained function in all right upper extremity muscles. Patient 2 spontaneously regained deltoid muscle function (Medical Research Council [MRC] to grade 3) at 6 months postinjury, eventually reaching MRC grade 5 deltoid strength over the next year along with full radial nerve function, including independent digital extension after nerve transfers. These imaging data were not used to alter clinical management.

4 | DISCUSSION

A crucial decision in management of traumatic BPI is whether to perform surgical intervention. The two cases described herein provide insights into how human nerves and MEPs respond to gunshot-induced BPI. The clinical course of both patients suggests that they sustained a reversible neurapraxia secondary to ballistic shock waves and subsequent soft-tissue swelling.[12,13] At the time of clinical presentation, electrodiagnosis and imaging could not distinguish between a pressure wave injury and irreversible axillary nerve damage.

There are animal data about the NMJ response to injury focused on terminal Schwann cells as well as molecular changes to the MEP, including the dispersion of acetycholine receptors.[14-18] Long-term denervation is accompanied by devolution of the MEP morphology from a mature "pretzel-like" appearance (perforated with membranous infoldings) toward an immature plaque

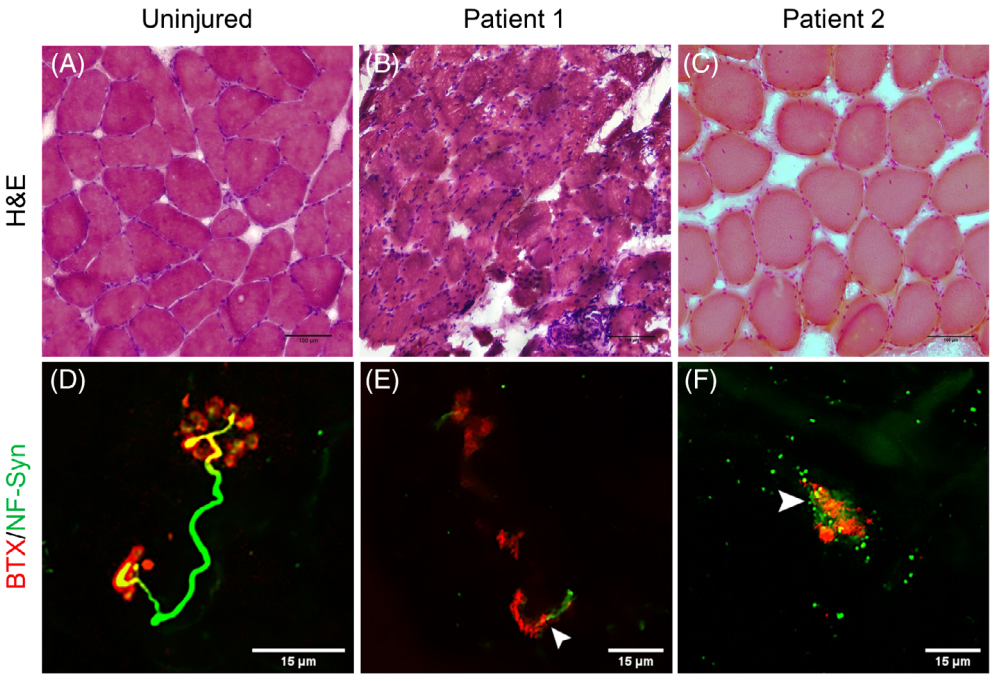

FIGURE 1 Deltoid muscle biopsies stained for (A-C) hematoxylin and eosin (scale bar = 100 µm) and (D-F) neuromuscular junction. Red = α-bungarotoxin; green = neurofilament and synaptophysin. White arrowheads denote direct contact of pre- and postsynaptic elements [Color figure can be viewed at wileyonlinelibrary.com]

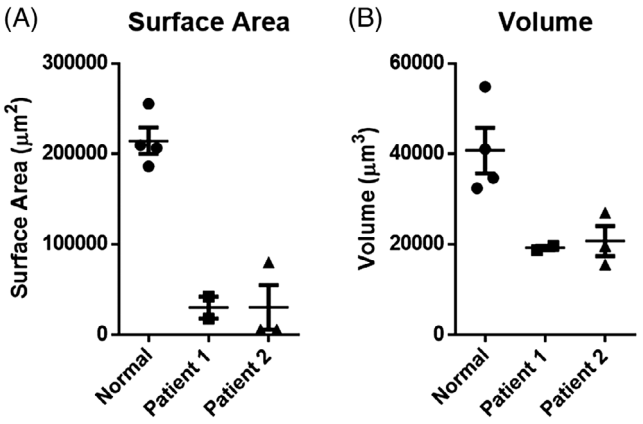

FIGURE 2 Quantification of motor endplate (A) surface area and (B) volume. Each data point represents one motor endplate from a single biopsy. Data are presented as mean ± standard error of the mean

(diminished size/increased density).[11] This transition to a plaquelike morphology is correlated with the critical time window beyond which reinnervation and functional recovery is severely limited. We used two-photon microscopy because it provides superior optical sectioning in three-dimensional imaging of thick human specimens when compared with standard confocal imaging.[19-21] The deeper penetration of two-photon excitation allows visualization and accurate quantification of morphometric parameters.[22,23] We observed significant neurofilament and synaptophysin debris in patient 1, suggesting active Wallerian degeneration, as would be expected 3 weeks after traumatic nerve injury.[24,25] MEP morphometric changes were evident in both patients, including decreases in surface area and volume, with increased density, consistent with the change to a plaquelike phenotype seen in murine models of traumatic nerve injury.[11,26] Taken together, these models show that such changes are reversible.[11]

Understanding the nature and time-course of changes in MEPs after nerve injury is critical to the development of an evidence-based decision process. However, these changes have not been studied in humans, and it is unknown whether the sequence of events and time-course are accurately represented by animal models. Biopsy of brachial plexus nerve fascicles has been undertaken for diagnosis of neuropathological states, but biopsy of denervated muscles and visualization of the MEPs has not been utilized.[27] Thus, our approach is a critical first step toward understanding these processes in humans. An understanding of the nature and time-course of degeneration of NMJs is also important for progressive neurodegenerative diseases. Denervation without motor neuron loss has also been implicated in the early stages of amyotrophic lateral sclerosis in both murine models and humans.[28] The late stages of chronic nerve compression have also been shown in animal models to resemble the sequelae of traumatic nerve injury.[29,30]

The major limitation of this preliminary study is its small sample size, so we cannot draw definitive conclusions about the nature and time-course of motor endplate remodeling or predict recovery and outcomes. In addition, we were able to perform biopsies in these patients because the muscle was easily accessible during surgical exposure for unrelated standard-of-care operations. If a separate procedure were required for muscle biopsy, the risks would have to be weighed against the benefits. Taking these considerations into account, our study has outlined a path for gathering evidence from muscle biopsy to complement electrodiagnostic and imaging modalities by precisely identifying the stages of NMJ degeneration in individual patients before surgery with the goal of helping to predict outcome.

CONFLICT OF INTEREST

The authors declare no potential conflicts of interest.

ETHICAL PUBLICATION STATEMENT

We confirm that we have read the Journal's position on issues involved in ethical publication and affirm that this report is consistent with those guidelines.

ORCID

Justin P. Chan https://orcid.org/0000-0002-2164-4724
Sameer B. Shah https://orcid.org/0000-0001-6613-3904
Ranjan Gupta https://orcid.org/0000-0002-8785-4900

REFERENCES

1. Kang JR, Zamorano DP, Gupta R. Limb salvage with major nerve injury: current management and future directions. *J Am Acad Orthop Surg*. 2011;19(suppl 1):S28-S34.
2. Lim SH, Lee JS, Kim YH, Kim TW, Kwon KM. Spontaneous recovery of non-operated traumatic brachial plexus injury. *Eur J Trauma Emerg Surg*. 2018;44:443-449.
3. Gupta R, Villablanca PJ, Jones NF. Evaluation of an acute nerve compression injury with magnetic resonance neurography. *J Hand Surg Am*. 2001;26:1093-1099.
4. Nwawka OK, Casaletto E, Wolfe SW, Feinberg JH. Ultrasound imaging of brachial plexus trauma in gunshot injury. *Muscle Nerve*. 2019;59:707-711.
5. Yoshikawa T, Hayashi N, Yamamoto S, et al. Brachial plexus injury: clinical manifestations, conventional imaging findings, and the latest imaging techniques. *Radiographics*. 2006;26(suppl):S133-S143.
6. Feinberg JH, Radecki J, Wolfe SW, Strauss HL, Mintz DN. Brachial plexopathy/nerve root avulsion in a football player: the role of electrodiagnostics. *HSS J*. 2008;4:87-95.
7. Noland SS, Bishop AT, Spinner RJ, Shin AY. Adult traumatic brachial plexus injuries. *J Am Acad Orthop Surg*. 2019;27:705-716.
8. Sulaiman W, Gordon T. Neurobiology of peripheral nerve injury, regeneration, and functional recovery: from bench top research to bedside application. *Ochsner J*. 2013;13:100-108.
9. Kurimoto S, Jung J, Tapadia M, et al. Activation of the Wnt/β-catenin signaling cascade after traumatic nerve injury. *Neuroscience*. 2015;294:101-108.
10. Palispis WA, Gupta R. Surgical repair in humans after traumatic nerve injury provides limited functional neural regeneration in adults. *Exp Neurol*. 2017;290:106-114.
11. Chao T et al. Matrix metalloproteinase 3 deletion preserves denervated motor endplates after traumatic nerve injury. *Ann. Neurol*. 2013;73:210-223.
12. Suneson A, Hansson HA, Lycke E, Seeman T. Pressure wave injuries to rat dorsal root ganglion cells in culture caused by high-energy missiles. *J Trauma*. 1989;29:10-18.

13. Volgas DA, Stannard JP, Alonso JE. Current orthopaedic treatment of ballistic injuries. *Injury*. 2005;36:380-386.
14. Reist NE, Werle MJ, McMahan UJ. Agrin released by motor neurons induces the aggregation of acetylcholine receptors at neuromuscular junctions. *Neuron*. 1992;8:865-868.
15. Kawabuchi M, Tan H, Wang S. Age affects reciprocal cellular interactions in neuromuscular synapses following peripheral nerve injury. *Ageing Res Rev*. 2011;10:43-53.
16. Kang H, Lichtman JW. Motor axon regeneration and muscle reinnervation in young adult and aged animals. *J Neurosci*. 2013;33:19480-19491.
17. Nicaise C, Frank DM, Hala TJ, et al. Early phrenic motor neuron loss and transient respiratory abnormalities after unilateral cervical spinal cord contusion. *J Neurotrauma*. 2013;30:1092-1099.
18. Kang H, Tian L, Thompson WJ. Schwann cell guidance of nerve growth between synaptic sites explains changes in the pattern of muscle innervation and remodeling of synaptic sites following peripheral nerve injuries. *J Comp Neurol*. 2019;527:1388-1400.
19. Pratt SJP, Iyer SR, Shah SB, Lovering RM. Imaging analysis of the neuromuscular junction in dystrophic muscle. *Methods Mol Biol*. 1687; 2018:57-72.
20. Pratt SJP, Shah SB, Ward CW, Kerr JP, Stains JP, Lovering RM. Recovery of altered neuromuscular junction morphology and muscle function in mdx mice after injury. *Cell Mol Life Sci*. 2015;72:153-164.
21. Deschenes MR, Hurst TE, Ramser AE, Sherman EG. Presynaptic to postsynaptic relationships of the neuromuscular junction are held constant across age and muscle fiber type. *Dev Neurobiol*. 2013;73: 744-753.
22. Denk W, Strickler JH, Webb WW. Two-photon laser scanning fluorescence microscopy. *Science*. 1990;248:73-76.
23. Akassoglou K, Merlini M, Rafalski VA, et al. In vivo imaging of CNS injury and disease. *J Neurosci*. 2017;37:10808-10816.
24. Beirowski B, Berek L, Adelbert R, et al. Quantitative and qualitative analysis of Wallerian degeneration using restricted axonal labelling in YFP-H mice. *J Neurosci Methods*. 2004;134:23-35.
25. Miledi R, Slater CR. On the degeneration of rat neuromuscular junctions after nerve section. *J Physiol*. 1970;207:507-528.
26. Marques MJ, Conchello JA, Lichtman JW. From plaque to pretzel: fold formation and acetylcholine receptor loss at the developing neuromuscular junction. *J Neurosci*. 2000;20:3663-3675.
27. Laumonerie P, Capek S, Amrami KK, Dyck PJB, Spinner RJ. Targeted fascicular biopsy of the brachial plexus: rationale and operative technique. *Neurosurg Focus*. 2017;42:E9.
28. Fischer LR, Culver DG, Tennant P, et al. Amyotrophic lateral sclerosis is a distal axonopathy: evidence in mice and man. *Exp Neurol*. 2004; 185:232-240.
29. Gupta R, Rowshan K, Chao T, Mozaffar T, Steward O. Chronic nerve compression induces local demyelination and remyelination in a rat model of carpal tunnel syndrome. *Exp. Neurol*. 2004;187: 500-508.
30. Chao T, Pham K, Steward O, Gupta R. Chronic nerve compression injury induces a phenotypic switch of neurons within the dorsal root ganglia. *J Comp Neurol*. 2008;506:180-193.

How to cite this article: Chan JP, Clune J, Shah SB, et al. Examination of the human motor endplate after brachial plexus injury with two-photon microscopy. *Muscle Nerve*. 2020;61:383–400. https://doi.org/10.1002/mus.26778

Identification of a homozygous *VRK1* mutation in two patients with adult-onset distal hereditary motor neuropathy

Lior Greenbaum MD, PhD[1,2,3] | Ortal Barel PhD[4] | Vera Nikitin MD[5] | Adi Hersalis-Eldar MD[5] | Nitzan Kol PhD[4] | Haike Reznik-Wolf PhD[1] | Dan Dominissini PhD[3,4] | Elon Pras MD[1,3] | Amir Dori MD, PhD[2,3,5]

[1]The Danek Gertner Institute of Human Genetics, Sheba Medical Center, Tel Hashomer, Israel

[2]The Joseph Sagol Neuroscience Center, Sheba Medical Center, Tel Hashomer, Israel

[3]Sackler Faculty of Medicine, Tel Aviv University, Tel Aviv, Israel

[4]Cancer Research Center and Wohl Institute for Translational Medicine, Sheba Medical Center, Tel Hashomer, Israel

Abstract

Background: Adult-onset hereditary motor neuropathies are caused by mutations in multiple genes. Mutations within the vaccinia-related kinase 1 (*VRK1*) gene were associated with a wide spectrum of recessively inherited motor neuropathies, characterized by childhood to early adulthood age of onset and an occasionally non-lower motor neuron involvement.

Abbreviations: CADD, combined annotation dependent depletion; CMA, chromosomal microarray analysis; CMAP, compound muscle action potential; CT, computed tomography; dHMN, distal hereditary motor neuropathy; dSMA, distal spinal muscular atrophy; EMG, electromyography; gnomAD, genome aggregation database; LRT, likelihood ratio test; MRI, magnetic resonanace imaging; NCS, nerve conduction studies; PCR, polymerase chain reaction; *VRK1*, vaccinia-related kinase 1; WES, whole-exome sequencing; WT, wild-type.